International Journal of Mass Spectrometry 284 (2009) 98–107

Contents lists available at ScienceDirect

International Journal of Mass Spectrometry

journal homepage: www.elsevier.com/locate/ijms

# Direct temperature mass spectrometric study on the depth-dependent compositional gradients of aged triterpenoid varnishes

Charis Theodorakopoulos[a,*], Jaap J. Boon[b], Vassilis Zafiropulos[c]

[a] Technological Educational Institute of Athens, Department of Conservation of Antiquities and Works of Art, Ag. Spyridonos, 122 10 Egaleo, Athens, Greece
[b] Foundation for Fundamental Research of Matter (FOM), FOM Institute for Atomic and Molecular Physics (AMOLF), Kruislaan 407, 1098SJ Amsterdam, The Netherlands
[c] Technological Educational Institute of Crete, Department of Human Nutrition & Dietetics, Ioannou Kondylaki 46, 723 00 Sitia, Crete, Greece

ARTICLE INFO

*Article history:*
Received 5 February 2008
Received in revised form 11 November 2008
Accepted 12 November 2008
Available online 21 November 2008

*Keywords:*
Triterpenoid varnish
Laser ablation
Gradient
Direct temperature-resolved mass spectrometry
Multivariant factor discriminant analysis

ABSTRACT

The depth profiles of aged dammar and mastic films, which were uncovered by optimized KrF excimer laser ablation (248 nm, 25 ns), were examined by direct temperature-resolved mass spectrometry (DTMS). The results establish the generation of depth-dependent compositional gradients in triterpenoid resins as a consequence of aging, for the first time on the molecular level. Electron ionization DTMS total ion currents show that the required temperature to volatilize the polar compounds and the relative amount of pyrolysis products of the high molecular weight condensed fraction is reduced when the upper layer of varying thickness of the films had been removed by the laser. The relative abundance of characteristic ion fragments of known oxidized triterpenoid compounds gradually decreased with depth. In contrast, the ion fragments of original resin molecules became more abundant with depth. The mass spectra of the bulk of the films resembled that of the control samples, which were not subjected to aging. Multivariant factor discriminant analysis quantified the oxidative gradients and showed that a depth of 15 μm from the surface of the aged films is the threshold between highly and much less deteriorated material.


## 1. Introduction

Triterpenoid (TTP) resins, such as dammar and mastic are known for the complexity of their composition incorporating more than 30 compounds based on the TTP skeleton [1–4] (Fig. 1). Aging of such resins is mainly due to ambient light and is in principle a side-chain oxidation process [4,5] (Fig. 2). Today, it is understood that aging of TTP-based coatings never ends, although the rate of degradation decreases in time. The on-going degradation process leads to radical cross-linking and condensation, oxidative modifications and shortening of the side-chains, especially of the dammarane skeleton compounds [2,3], and to eventual defunctionalization and disintegration of the TTP carbon skeleton [6].

The extent of oxidative degradation is significantly affected by the UV wavelengths in the ambient light. Oxidation under visible light proceeds by functionalization of oleanane and ursane type TTP compounds at positions C-11 and C-28 [2] (Fig. 2b). UV-including light leads to opening of the A-ring and additional oxidation at position C-2 of dammarane and oleanane/ursane type molecules [7] (Fig. 2c). To date there are various reports showing that UV light aging is essential for the study of extremely aged TTP varnishes [7–10]. Besides, during harvest the TTP resin teardrops are left to dry under sunlight straight after exudation from the bark of the resin trees [11], initiating free radical chain reactivity prior to any further manipulation [12]. As a result, freshly harvested TTP resins already contain dammarenolic acid and 20,24-epoxy-25-hydroxy-dammaran-3-one [13,14] both having oxidized A-rings [2,3,5,10].

A recent study, based on ultraviolet–visible (UV/vis) spectrophotometry and attenuated total reflection (ATR) Fourier transform infrared (FT-IR) spectroscopy, demonstrated that carbonyl groups reduce as a function of depth in TTP films exposed to accelerated aging as a consequence of reducing absorption with increasing light wavelengths [15]. The latter study showed that ambient UV wavelengths are completely absorbed at the uppermost few microns from the surface of such films. Owing to the strong light intensity and the availability of oxygen in the surface, most of the oxidative products must be generated in the surface, while the limited availability of oxygen in the bulk should result in termination reactions of free radicals producing non-oxidative cross-links, as indicated by gas chromatography–mass spectrometry (GC/MS) [6]. There are further studies indicating that thickness plays a significant role in the aging profile of such varnishes. Aged dammar films thicker than 10 μm were found to be less deteriorated than thinner films aged under the same protocol [8]. It was shown elsewhere that the optical densities of a wide range of light-aged dammar films increased with

* Corresponding author. Tel.: +30 210 5385407; fax: +30 210 5385406.
*E-mail address:* ctheodlos@teiath.gr (C. Theodorakopoulos).

1387-3806/$ – see front matter © 2008 Elsevier B.V. All rights reserved.
doi:10.1016/j.ijms.2008.11.004

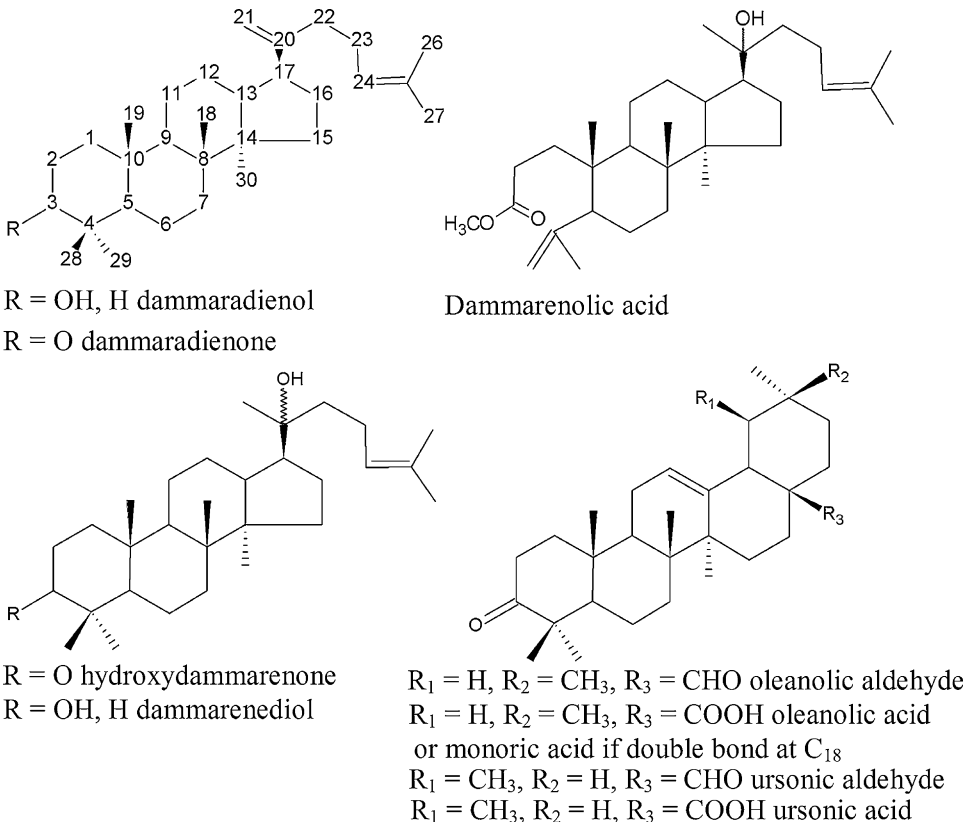


**Fig. 1.** Triterpenoid (TTP) molecular compounds of dammar and mastic resins. Dammarane type TTPs are more abundant in dammar, whereas oleanane/ursonic type TTPs are more abundant in mastic.

decreasing thickness [16]. Solubility tests across the depth profile of naturally aged 19th century TTP varnishes showed that polarity decreases as a function of depth [17]. Continuous wave electron paramagnetic resonance (cw-EPR) showed that the amount of free radicals in fresh mastic resin teardrops increases as the teardrops (all harvested in the same period) decrease in size [12]. Monitoring of the depth profiles of aged TTP resins by ATR/FT-IR demonstrated the presence of depth-dependent gradients in methylene species, implying that condensation and ring disintegration of the TTP compounds reduce as a function of depth [15]. It is therefore solidly indicated that deterioration of aged triterpenoids coatings reduces with depth from surface.

These findings are supported by theoretical models on the aging of various organic materials. There are early hypotheses on the presence of "unreacted substance" across depth of light-aged organic films [18] and postulations, based on Beer's Law, suggesting that the abundance of this unreacted material should increase with increasing distance from surface [19,20]. Some models implied that the consumption of oxygen across depth is dependent upon a reducing rate of diffusion, which leads to 'oxygen starvation' in the bulk [20–22]. The integration of data resulting from reducing light propagation into films and from the reduction of oxygen availability with depth produced further models showing that the overall degradation of organic substrates is reduced as a function of depth [23]. A comprehensive review on depth-dependent degradation indications in various materials due to light propagation and oxygen diffusion has been already available [24].

This paper provides for the first time direct experimental evidence of the occurrence of compositional gradients across the thickness of aged dammar and mastic varnishes on the molecular level. The depth profile of accelerated aged dammar and mastic was uncovered by optimized KrF excimer laser ablation that enabled the formation of successive depth steps across the thickness of the films [17,25,26]. There was previous strong evidence that there is no oxidative contribution of the 248 nm pulsed laser to the remaining films after parameter optimization [27]. The following work is based on direct temperature-resolved MS (DTMS) of the remaining coatings below each depth-step. Analytical data from earlier studies on TTP resins, based on high performance liquid chromatography MS (HPLC/MS), GC/MS and DTMS, were employed for the optimum interpretation of the DTMS results [2,5,10,28]. Quantification of the DTMS data was enabled by multivariant factor (MF) discriminant analysis (DA).

## 2. Experimental

### 2.1. Materials

Fresh TTP mastic and dammar resin fragments were diluted in xylene 40% (w/v) and spin-coated on a Headway Research® I-PM-1010D-CB15 Spinner at 250–1000 rpm on quartz sheets to produce 55 μm thick films. After drying, aging was accelerated in a Sunset CPS, Heraeous® xenon-arc fadeometer. Wavelengths longer than 295 nm were employed to imitate sunlight exposure. The films received a cumulative light dose of 160 Mlx h and were then exposed to open air for 45 days followed by 30 days of storage in the dark.

### 2.2. Processing

A Lambda Physik®, COMPex series, KrF excimer laser ($\lambda$ = 248 nm) was used with a pulse duration of 25 ns and maximum source energy of 300 mJ per pulse to fabricate depth-step zones onto the films tested. For optimum control of the laser–film inter-

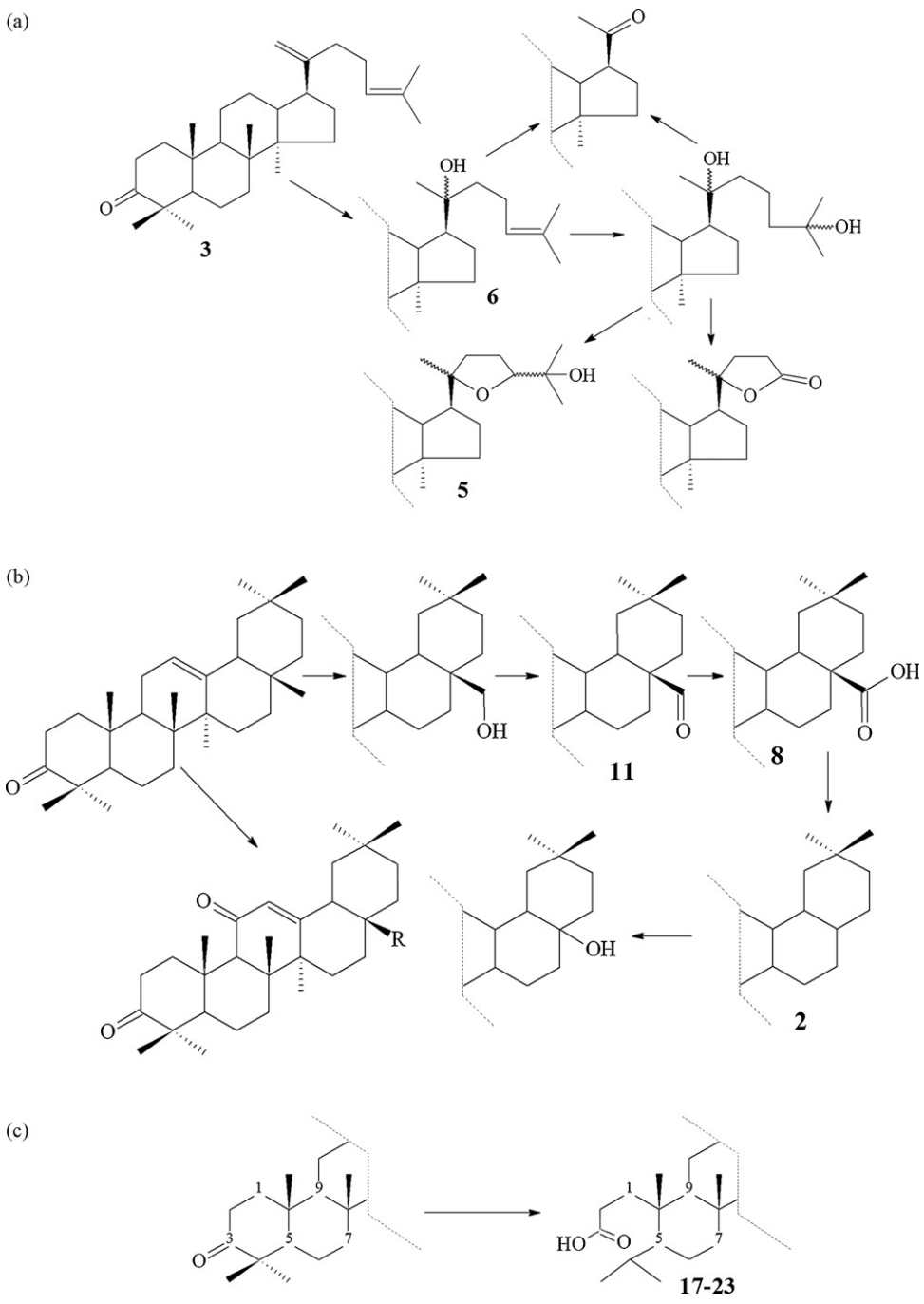


**Fig. 2.** Oxidation stages of: (a) dammarane type molecules in the side-chain, (b) oleanane-type molecules and (c) the A-ring at position C-2 of dammarane type molecules [2–4,31]. The figures correspond to labels in Table 1.

action, laser ablation rate studies were performed to determine the optimum laser fluence [26,29,30] for the ablation of each case [25]. The final etching depths were determined using a mechanical profilometer (Perthometer® S5P). "Laser cleaning" was performed by scanning adjacent areas of the films with a pre-calculated number of laser pulses across the Gaussian profile of the laser beam [17,25]. This process resulted in the formation of depth-step zones (Fig. 3) of cumulative 3.5, 7, 11.5, 15, 17, and 25 μm in dammar and 3, 6, 10, 12, 16, 20, and 25 μm in mastic films of approximately 55 μm thickness. Including the degraded surfaces of the films and the control samples ('unaged' coatings), this processing generated eight to nine sampling steps in the 55 μm thick dammar and mastic films, respectively.

### 2.3. Direct temperature-resolved mass spectrometry

The sampling depth steps were examined by DTMS in order to investigate the potential molecular variation across the depth profile of the films. From each step the remaining film of approximately 4 $mm^2$ was removed, then homogenized and brought in suspension with a few drops of ethanol. A volume of 2–3 μl of the mixture was applied to a Pt/Rh (9:1) filament (100 μm diameter) of a direct insertion probe, and dried *in vacuo* by evaporation of the ethanol. After insertion of the probe in the ionization chamber, the filament was resistively heated by ramping the current at a rate of 1 A/min. Using this ramp the temperature was linearly increased from ambient to approximately 800 °C in 2 min, while the MS was monitoring the

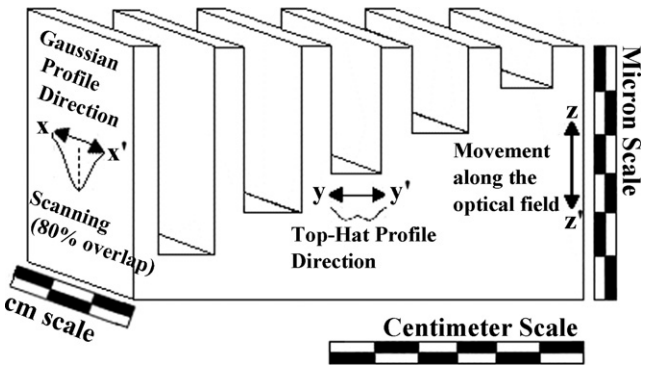


**Fig. 3.** Representation of the depth-step zones etched on the films by a KrF excimer laser (248 nm, 25 ns). The resin depth along the *zz′* axis of the optical field of the laser has been exaggerated. The orientations of the Gaussian (*xx′*) and top-hat (*yy′*) laser beam profiles are shown.

evolved compounds in electron ionization (EI) or ammonia chemical ionization ($NH_3$/CI) modes. The compounds were ionized at 16 eV energy in EI mode and 250 eV in $NH_3$/CI mode, and analyzed in a JEOL SX-102 double focusing mass spectrometer (B/E) over a mass range from 20 to 1000 Da at a cycle time of 1 s. The acceleration voltage was 8 kV. The total ion currents and sum mass spectra (all mass spectra summed over the entire scan range) were examined. Interpretation was assisted by earlier DTMS studies [2,4,10,31], as well as GC/MS and HPLC–MS data [2,3].

### 2.4. Multivariant factor discriminant analysis (MF-DA)

EI-DTMS sum mass spectra were numerically analyzed by factor discriminant analysis coupled with the FOMpyroMAP multivariate analysis program, that is a modified version of the ARHTUR package from Infometrix Inc. (Seattle, USA; 1978 release), and with a FOM developed Matlab® (The Mathworks Inc., Natick, MA, USA) toolbox ChemomeTricks. The discrimination was based on a double stage principal component analysis (PCA) [32] using sum mass spectra of sample analyzed in triplicate. To minimize variance in the data due to day-to-day variance in the instrument performance and sample handling, all DTMS spectra of the same films were measured on the same day.

## 3. Results and discussion

DTMS is based on thermally assisted volatilization and pyrolysis for rapid analysis of complex molecular systems and requires minor sample quantities without prior chemical processing [33]. The low voltage ionization utilized minimizes electron-induced ionization while ammonia chemical ionization is used to determine molecular weight. More than 30 TTP molecules of moderate molecular weight (MW: 400–500 Da) have been identified in degraded dammar and mastic films by DTMS [2,4,10,31]. Because of the sampling and the subsequent dissolution in ethanol of the samples tested by DTMS, the final MS data are average readings with respect to the abundance of the identified compounds across depth. During DTMS runs the ionized components are separated in apolar, polar and cross-linked fractions that desorb in increasing temperature windows up to 800 °C [33]. Once the thermally dissociated products are formed, evaporation occurs instantly under vacuum and, hence, there is minor possibility of secondary reactions due to molecular collisions. The apolar and polar fractions desorb at relatively low temperatures via evaporation, while high MW cross-linked material desorbs at higher temperatures via pyrolysis. These groups generate distinctive peaks in the order of the temperature of desorption and are monitored in the DTMS total ion currents (TIC).

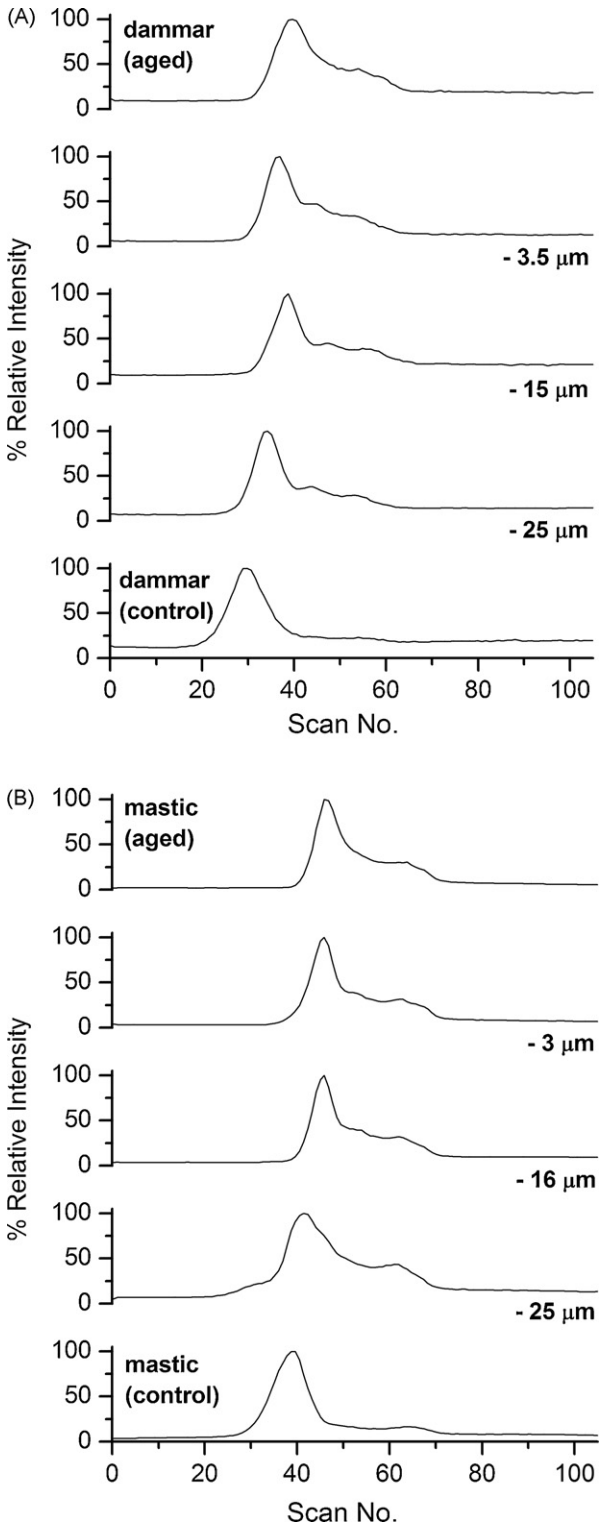


**Fig. 4.** EI-DTMS TIC's of laser-ablated depth steps of aged dammar (a) and mastic (b).

Consequently, the upper EI-DTMS TIC spectra in Fig. 4 indicate the increase in polarity and cross-linking in the accelerated aged TTP films [4,10].

### 3.1. DTMS of the control (unaged) TTP films

The $NH_3$/CI-DTMS sum mass spectra of two varnishes are shown in Fig. 5. Figs. 6 and 7 show the corresponding EI-DTMS spectra. The

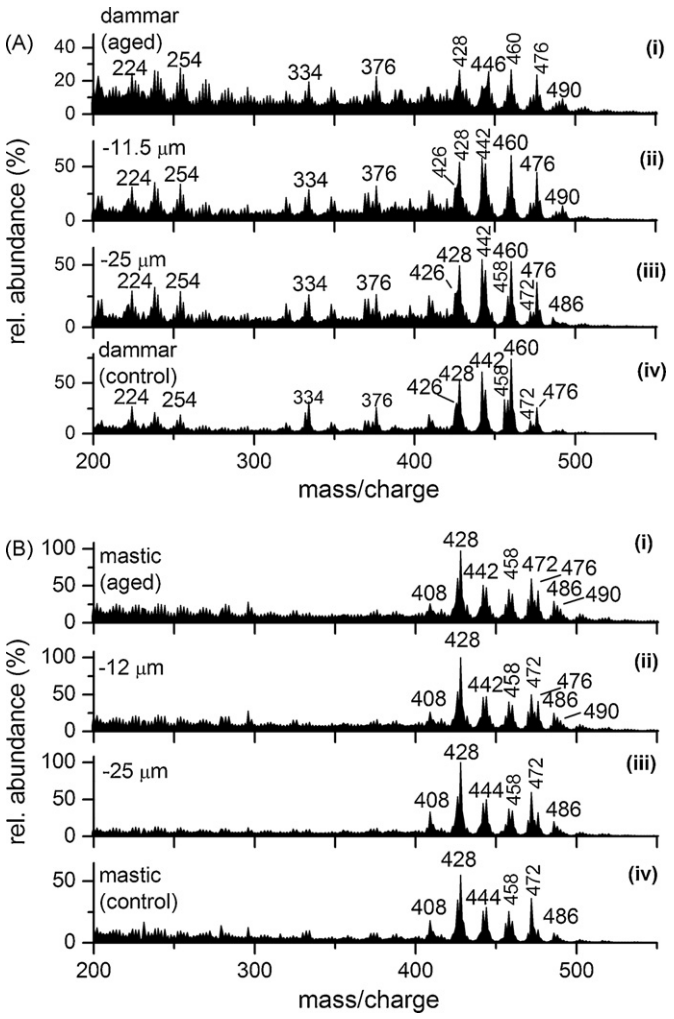


**Fig. 5.** NH3/CI DTMS sum mass spectra at selected depth steps and the controls of the accelerated aged dammar (a) and mastic (b).

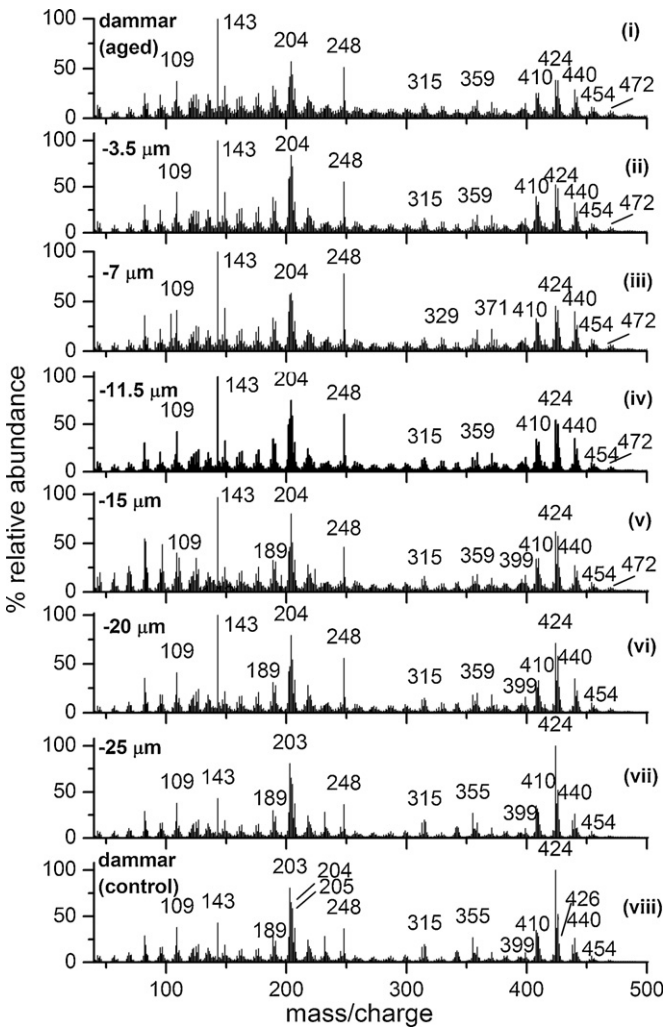


**Fig. 6.** EI-DTMS sum mass spectra of the aged dammar film (55 μm thickness) (i), and the depth steps at 3.5 μm (ii); 7 μm (iii); 11.5 μm (iv); 15 μm (v); 20 μm (vi); 25 μm (vii) from surface as well as the control film (viii).

compounds detected are listed in Table 1. Under EI ionization minor fragmentation of the incorporated molecules is induced, thereby yielding structural and hence more detailed information, whereas under $NH_3$/CI ionization mode ammonia adduct molecular ions $[M+NH_4]^+$, $[M+H]^+$ and $[M+NH_4-H_2O]^+$ cations are obtained, thus giving MW information. The EI-DTMS sum mass spectra of both control films have a high abundance of mass/charges between *m*/*z* 400 and 500, attributed to TTP molecular ions and radical cations $[M-H_2O]^{\cdot+}$ [2,10], which reflect the MW of TTP molecules.

From this point on the numbers in bold in the text refer to the compounds listed in Table 1. Relative abundances of EI *m*/*z* 204 and 410 and $NH_3$/CI *m*/*z* 428 indicate the presence of nor-α-amyrone (**1**) and/or nor-β-amyrone (**2**) in dammar [3,5], but only nor-β-amyrone (**2**) in mastic [3,34]. The presence of dammarane type molecules, i.e., dammaradienone (**3**) [5,13,35], dammaradienol (**4**) [5,13,14,35], dammarenolic acid (**5**) and hydroxydammarenone (**6**) [5,13,14] that are present in fresh dammar films [2,3,10], is also detected. Characteristic components with the dammarane skeleton are present in unaged mastic, i.e., **3** and **6**, in line with earlier findings [2,3,10,28,34]. The EI-DTMS spectra of dammarane type molecules have a common ionic fragment at *m*/*z* 109 resulting from aliphatic side-chain scission at position C-17 of the dammarane skeleton [3]. The presence of **3** and **6**, which have additional ion peaks at EI *m*/*z* 424 ($[M]^{\cdot+}$), 205 and *m*/*z* 315, 355, 424 ($[M-OH]^+$) respectively and the same ion peaks at $NH_3$/CI *m*/*z* 442 ($[M+NH_4]^+$ corresponding to **3** and $[M-OH+NH_4]^+$ to **6**), indicates the molecular similarities of dammar and mastic. However, dammarane compounds are more abundant in dammar as found elsewhere [2,10].

In contrast, oleanane molecules are more abundant in mastic than in dammar [2,10]. The ionic fragments of oleanonic and ursonic acids and aldehydes **8**, **9**, **11**, **12** are detected in dammar [5,13,14] and the oleanane-type compounds **8**, **10**, **11** in mastic [2,10]. Ursane type TTP molecules, i.e., **8**, **10** and **11**, are not present in mastic [28,34]. A good marker for identification of mastic is the moronic acid, **10** [1], which has the same MW and ionic fragments as oleanolic acid, **8**. Mastic also has additional compounds, such as (iso)masticadienonic acid, **13** [28,36], with reported EI *m*/*z* 439, 454 and $NH_3$/CI *m*/*z* 472 [10], and 3-O-acetyl-3-epi(iso)masticadienonic acid, **14** [28], corresponding to a low relative abundance at EI *m*/*z* 438, 498, $NH_3$/CI *m*/*z* 516 (not shown). However the ion peaks of **13** coincide with those of compounds **8**–**10** and the ion peaks of **14** coincide with those of compounds **11**, **12** [10]. In contrast the ionic fragments of 28-nor-olean-18-en-3-one, **16**, at EI *m*/*z* 163 and 191 are a clear marker of mastic resin [10].

Judging from earlier findings, both TTP resins examined here were somewhat oxidized before aging. Dammarenolic acid, **5**, has been indicated to be the major acidic constituent in dammar [13]. This molecule has a carboxylic acid group at position C-2, which

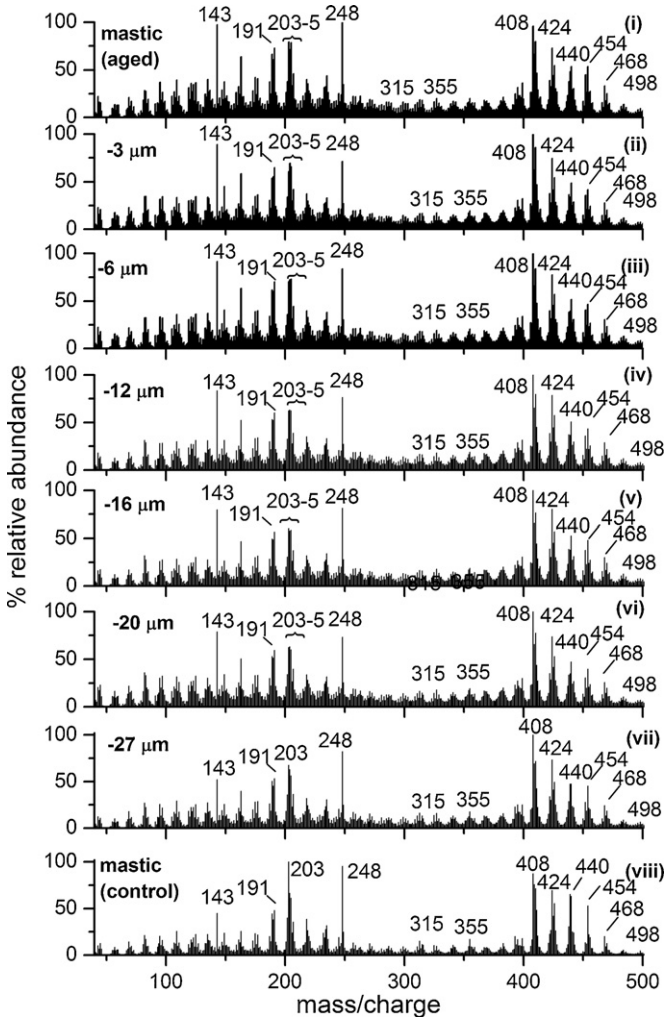


**Fig. 7.** EI-DTMS sum mass spectra of the aged mastic film (55 μm thickness) (i), and after removal of 3 μm (ii); 6 μm (iii); 12 μm (iv); 16 μm (v); 20 μm (vi); 27 μm (vii) from surface as well as the control film (viii).

results from A-ring opening of the dammarane skeleton and derives from oxidation of **6**. The sum mass spectra of the control mastic film indicate the presence of **5**, by the EI ion peak at *m*/*z* 440, $[M-OH]^+$ and the $NH_3$/CI *m*/*z* 458 and 476 corresponding to the ammonia adducts of the former ionic fragment and the molecular ion of **5**, $[M-OH+NH_4]^+$ and $[M+NH_4]^+$. The mass spectra of both resins determine the presence of the ocotillone compound **7**, which derives from oxidation of dammarane skeleton molecules with a hydroxyl-isopropyl-methyl-tetra-hydro-furan side-chain signified by the ionic fragment at *m*/*z* 143 in both EI and $NH_3$/CI modes [2]. HPLC/MS analysis of dammar has determined the presence of dammarane type degradation compound **15** that has both the A-ring oxidation site and the ocotillone group [3]. Compound **15** that is not present in fresh mastic [2], was recently detected in fresh dammar resin by DTMS [10].

The presence of oxidized dammarane type TTP compounds at an early degradation stage of the resins, is attributed to the presence of free radicals generated by sunlight exposure during exudation from the bark of the resin tree [11,12]. Oxidized 'fresh' TTP resins have also been detected by graphite-assisted laser desorption/ionization (GALDI) MS [9]. Traces of some cross-linked oligomers of polycadinene, the polymer of dammar [37], and cis-1,4-poly-β-myrcene, the polymer of mastic [38], are obvious by mass increments of 204 Da in dammar and 136 Da in mastic. In line with a previous DTMS study [10], sequences of 16 Da increments starting at the molecular ions mono- to tetra-mers of cadinene (EI *m*/*z* 204, 408, 612 and 816) in dammar and mono- to penta-mers of poly-β-myrcene (EI *m*/*z* 136, 272, 408, 544, 680 and 816) in mastic indicated oxidation of polymerized TTP molecules in both cases [25]. The low relative abundance of fragments of oxidized compounds and the high relative abundance of fragments corresponding to original TTP molecules (**1**–**16** depending on the resin), indicate that both resins kept most of their original molecular signatures.

### 3.2. DTMS of the TTP films exposed to accelerated aging

The EI-DTMS TIC's show that both films became less volatile owing to increased degrees of polarity and cross-linking after accelerated aging (Fig. 4). The EI sum mass spectra of the aged films reveal a reduction in the relative abundance of the ionic fragments of dammarane (**3**–**7**) and oleanane/ursane compounds (**1**, **2**, **8**–**10**) with marker peaks at EI *m*/*z* 424 and 440 for the dammarane, *m*/*z* 204, 410 (**1**, **2**), *m*/*z* 454 ($[M]^{\cdot+}$ of **8**–**10**) and *m*/*z* 438 ($[M]^{\cdot+}$ of **11**, **12**) for the oleanane/ursane type of molecules. The reduction in abundance is less intense in mastic (Fig. 7), as also reported elsewhere [2,4,10].

In both aged films, EI *m*/*z* 143, 399 and $NH_3$/CI *m*/*z* 143, indicate the presence of ion fragments of oxidized dammarane molecules with the ocotillone side-chain, i.e., **7**, **15**. In mastic, no oxidation products are known for compounds **13**, **14**. It has been suggested that these compounds are involved in cross-linking concluded from mass/charges at *m*/*z* 900, which could point to dimerized **13** molecules [10].

Both films show an abundance of peaks of moderate relative intensity corresponding to compounds **17**/**18**, **19**/**20** and **21** for dammar and **18**/**22**, and **20**/**23** for mastic, identified by their molecular ions $[M]^{\cdot+}$ at EI *m*/*z* 428, 460 and 472 and the ammonia adduct ions $[M+NH_4]^+$ at $NH_3$/CI *m*/*z* 446 and 490. These secondary products have been identified in xenon arc exposed dammar under UV-including light [7,10]. In dammar, compound **21** is similar to compound **5** indicating its dammarane skeleton origin. The difference between the two compounds lies in position C-5, at which **21** has an isopropyl group and **5** an isopropenyl group [7]. These degraded molecules have oxidized A-rings at C-2 (Fig. 2c) [4,7]. The DTMS spectra include peaks at *m*/*z* 204 for **17**, **18**, **22** and *m*/*z* 203 for **19**, **20**, **23** [4]. Compounds with these ion fragments are also present in fresh TTP resins. For example, **1** and **2** have an ion fragment peaking at *m*/*z* 204 that is characteristic of the oleanane and ursane skeleton with a hydrogen at position C-17, while **8**–**12** have an ion fragment peaking at *m*/*z* 203 corresponding to the oleanane/ursane skeleton oxidized at C-17 [4]. These products **17**–**20**, **22** and **23** derive from oleanane and ursane TTPs, whose oxidation has been attributed to Norrish type I reactions [8,31,39]. Such degradation compounds are not formed in TTP varnishes protected in UV-free environments [4,7]. However, exposure under UV wavelengths has been often utilized for the study of TTP films [7–10]. As mentioned above, even prior to aging both TTP films have a relatively high abundance of compounds **5**, **7** and **15** (dammar only) with oxidized A-rings [5,13,14]. These compounds may be formed during the resin biosynthesis or by sunlight during excretion from the resin tree bark [12] and therefore the presence of A-ring oxidized "seco" compounds **17**–**23** indicates an advanced degree of degradation of such resins.

In addition, other oxidation products are recognized from their characteristic ion peaks in the EI mode. These are compounds **24**–**28** in dammar and **24**–**26** in mastic. Compound **24** is the only one derived from dammarane type molecules. Compounds **25**–**28** derive from oxidation of TTPs with the oleanane and ursane skeleton [2]. These products were reproduced under UV-free light and by artificial aging in solution under fluorescent light [31].

**Table 1**
Identified compounds across the depth profiles of the TTP dammar and mastic resin films.

| Label | Compound name | Mw | EI mass/charges[a] | $NH_3$/CI mass/charge | Dammar | Mastic |
|---|---|---|---|---|---|---|
| **1** | Nor-α-amyrone (3-oxo-28-nor-urs-12-ene) | 410 | **204**, 410 | 428 | Control, aged (bulk) | N/A |
| **2** | Nor-β-amyrone (3-oxo-28-nor-olean-12-ene) | 410 | **204**, 410 | 428 | Control, aged (bulk) | Control, aged (bulk) |
| **3** | Dammaradienone (3-oxo-dammara-20(21),24-diene) | 424 | 109, 205, **424** | 442 | Control, aged (bulk) | Control, aged (bulk) |
| **4** | Dammaradienol (3β-hydroxy-dammara-20,24-diene) | 426 | **109**, 189,207,408, 426 | 444 | Control, aged (bulk) | N/A |
| **5** | Dammarenolic acid (20-hydroxy-3,4-seco-4(28),24-dammaradien-3-oic acid) | 458 | **109**, 440 | 476,458 | Control, aged (bulk) | Control, aged (bulk) |
| **6** | Hydroxydammarenone (20-hydroxy-24-dammaren-3-one) | 442 | 109, 315, 355, **424** | 442 | Control, aged (bulk) | Control, aged (bulk) |
| **7** | 20,24-epoxy-25-hydroxy-dammaran-3-one | 458 | **143**, 399 | 143 | Control, aged (bulk) | Control, aged (bulk) |
| **8** | Oleanonic acid (3-oxo-olean-12-en-28-oic acid) | 454 | 189, **203**,248,409, 454 | 472 | Control, aged (bulk) | Control, aged (bulk) |
| **9** | Ursonic acid (3-oxo-12-ursen-28-oic acid) | 454 | 189, **203**,248,409, 454 | 472 | Control, aged (bulk) | N/A |
| **10** | Moronic acid (3-oxo-olean-18-en-28-oic acid) | 454 | **189**, 203,248,409, 454 | 472 | N/A | Control, aged (bulk) |
| **11** | Oleanonic aldehyde | 438 | **203**, 232, 409, 438 | 456 | Control, aged (bulk) | Control, aged (bulk) |
| **12** | Ursonic aldehyde | 438 | **203**, 232, 409, 438 | 456 | Control, aged (bulk) | N/A |
| **13** | (Iso)masticadienonic acid (3-oxo-13α,14β,17βH,20αH-lanosta-8,24-dien-26-oic acid or 3-oxo-13α,14β,17βH,20αH-lanosta-7,24-dien-26-oic acid) | 454 | 439, **454** | 472 | N/A | Control, aged (bulk) |
| **14** | 3-O-acetyl-3-epi(iso)masticadienolic acid (3α-acetoxy-13α,14β,17βH,20αH-lanosta-8,24-dien-26-oic acid or 3α-Acetoxy-13α,14β,17βH,20αH-lanosta-7,24-dien-26-oic acid) | 498 | **438**, 498 | 516 | N/A | Control, aged (bulk) |
| **15** | 20,24-Epoxy-25-hydroxy-3,4-seco-4(28)dammaren-3-oic acid | 474 | 143 | 143 | Control, aged | Control, aged |
| **16** | 28-Nor-olean-18-en-3-one | 410 | 163, 191, 410 | 428 | N/A | Control, aged (bulk) |
| **17** | 3,4-Seco-28-nor-urs-12-en-3-oic acid | 428 | 204, 428 | 446 | 0–15 μm | N/A |
| **18** | 3,4-Seco-28-nor-olean-12-en-3-oic acid | 428 | 204, 428 | 446 | 0–15 μm | 0–15 μm |
| **19** | 3,4-Seco-28-nor-urs-12-en-3,28-dioic acid | 472 | 203, 248 472 | 490 | 0–15 μm | N/A |
| **20** | 3,4-Seco-28-nor-olean-12-en-3,28-dioic acid | 472 | 203, 248 472 | 490 | 0–15 μm | 0–15 μm |
| **21** | Dihydro-dammarenolic acid (20-hydroxy-3,4-seco-24-dammaren-3-oic acid) | 460 | 387, 456 | 478 | 0–15 μm | N/A |
| **22** | 3,4-Seco-28-nor-olean-18-en-3-oic acid | 428 | 204, 428 | 446 | N/A | 0–15 μm |
| **23** | 3,4-Seco-28-nor-olean-18-en-3,28-dioic acid | 472 | 203, 248 472 | 490 | N/A | 0–15 μm |
| **24** | 3-Oxo-25,26,27-trisnordammarano-24,20-lactone | 414 | 95, 99, 205, 315, **414** | 432 | 0–55 μm, control (tr) | 0–55 μm, control (tr) |
| **25** | 17-Hydroxy-11-oxo-nor-β-amyrone (3,11-dioxo-17-hydroxy-28-norolean-12-ene) | 440 | **234**, 275, 422, 440 | 458 | 0–55 μm, control (tr) | 0–55 μm, control (tr) |
| **26** | 11-Oxo-oleanonic acid (3,11-dioxo-olean-12-en-28-oic acid) | 468 | 217, 257, **276**, 317, **482** | 486 | 0–55 μm, control (tr) | 0–55 μm, control (tr) |
| **27** | 17-Hydroxy-11-oxo-nor-α-amyrone (3,11-dioxo-17-hydroxy-28-norurs-12-ene) | 440 | **234**, 275, 422, 440 | 458 | 0–55 μm, control (tr) | N/A |
| **28** | 11-Oxo-ursonic acid (3,11-dioxo-urs-12-en-28-oic acid) | 468 | 257, 276, **317**, **482** | 486 | 0–55 μm, control (tr) | N/A |

[a] *m*/*z* in bold correspond to the highest relative intensity of the series according to previous findings [2].

A comparison of the relative abundance of the characteristic ion fragments of both UV and non-UV-induced types of oxidation products indicates that they are almost in equal amounts in both films (Table 2). The composition of the examined degraded varnishes is a mixture of (a) intact TTP compounds: **1**–**16** (unreacted material), (b) UV-induced oxidized compounds (**17**–**23**) and (c) non-UV oxidized compounds (**24**–**28**). There is significant evidence that UV-induced and non-UV oxidation as well as non-oxidative degradation occur across the depth profile of aged TTP coatings as a result of a depth-dependent optical gradient determined by UV/VIS spectrophotometry [15].

### 3.3. DTMS across depth into the accelerated aged TTP films

The EI-DTMS-TIC's of both films, and especially of the evaporated volatile fraction, show shifts towards lower scan numbers across the successive depth steps, demonstrating that the temperature required for sufficient desorption decreases with depth (Fig. 4). Consequently, the thinner the varnishes were left after laser ablation the more volatile the remaining films were detected by the MS analysis. The shifts of the TIC curves indicate that after removal of 20 and 25 μm from the aged dammar and mastic films respectively, evaporation of volatiles requires less heat compared to the

**Table 2**
UV-induced versus non-UV-induced oxidized compounds in aged dammar and mastic films.

| | UV-induced oxidized compounds | | | Non-UV-induced oxidized compounds | | |
|---|---|---|---|---|---|---|
| | Label | Characteristic EI *m*/*z* | Relative abundance (%) | Label | Characteristic EI *m*/*z* | Relative abundance (%) |
| Dammar (*m*/*z* 143, 100% relative abundance) | **17/18** | 428 | 13.4 | **24** | 414 | 9 |
| | **19/20** | 472 | 6.4 | **25/27** | 234 | 12 |
| | **21** | 456 | 10.9 | **26** | 482 | 3.3 |
| | | | | **28** | 317 | 9.3 |
| Mastic (*m*/*z* 248, 100% relative abundance) | **18/22** | 428 | 26.9 | **24** | 414 | 21.5 |
| | **20/23** | 472 | 14.9 | **25** | 234 | 32.3 |
| | | | | **26** | 482 | 11.7 |

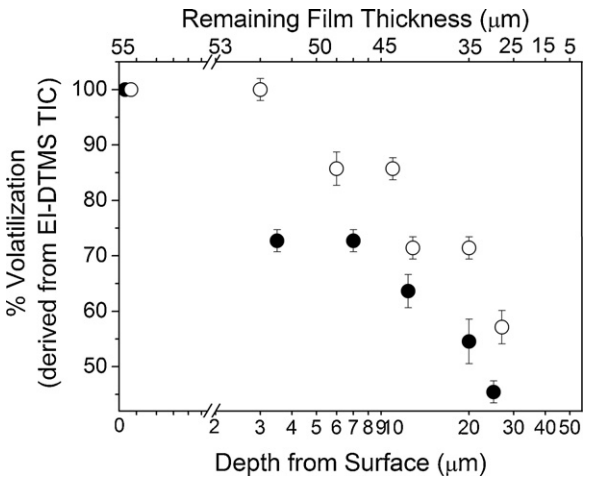


**Fig. 8.** The outlined gradients in volatilization in the EI-DTMS TIC plots across the depth profiles of the accelerated aged dammar (●) and mastic (○) films.

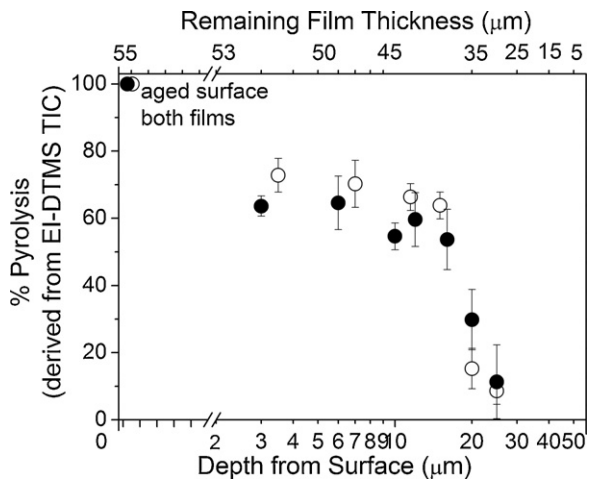


**Fig. 9.** The outlined gradients derived from the integrated areas of the pyrolysis yield in the EI-DTMS TIC plots across the depth profiles of the accelerated aged dammar (●) and mastic (○) films.

aged films. These shifts clearly correspond to the depth-dependent gradients in polarity [17] and the gradual reduction of the concentration of carbonyl groups with depth [15]. In both films, pyrolysis of the high MW fraction occurs at about the same temperatures but the TIC profiles indicate changes in relatively amount of cross-linked material with depth. The depth-dependent gradients in MW in TTP films have been confirmed by HP-SEC [25]. According to the EI-DTMS TICs then, the accelerated aging of TTP films led to reducing degrees of oxidation, polarity and cross-linking as a function of depth.

Fig. 8 shows the percentage of the shifts of the volatilization peaks in the TIC plots, when the scan number of volatilization apexes of the aged films prior to laser ablation was set as maximum (100%) and the volatilization apexes of the unaged films (controls) as minimum (0%), against the logarithm of the laser-ablated depth steps (Table 3). These plots quantify the polarity shifts as derived from the EI-DTMS TIC curves. The gradient in the high MW fraction versus depth is demonstrated by the plots based on the area integrals of the pyrolysis peak of the EI-DTMS TIC curves (Fig. 9). The latter show two trends in the TTP films. The first trends are terminated at approximately 15 μm from surface, where there is an apparent change in slope of the delineated curves, after which new trends commence till the degree of pyrolysis becomes similar to that prior to aging in both cases. The leap shown in the curves after the 15 μm step coincides with changes in the ablation behavior of the films [25], implying that at this particular depth there is also a change in the interaction of the films with the 248 nm laser pulses [29,40,41]. The data imply that at depths exceeding 15 μm surfaces neither of the aged TTP films was heavily oxidized and cross-linked.

The sum MS data show indeed that the thinner the films left by the laser, the more the molecular configuration of the remaining films tends to resemble the composition of the resins prior to aging (Figs. 5–7). The depth-dependent shift towards a less oxidative state is evident even at the first depth-step at depths of only 3.5 and 3 μm in the aged dammar and mastic films, respectively. The unreacted compounds observed are the dammarane type TTPs (**3**–**7**) at EI *m*/*z* 109, 143, 424 and $NH_3$/CI *m*/*z* 442, 446, 478 and the oleanane/ursane TTPs (**1**, **2**, **8**–**12**) at EI *m*/*z* 189, 203, 204, 248, 409, 410 and $NH_3$/CI *m*/*z* 428, 456, 472. The recovery of the ion fragments corresponding to these marker compounds is higher in dammar, because of the abrupt reduction of the TTP compounds in dammar upon aging [2,4,10].

The UV-induced oxidized compounds **17**/**18**, **19**/**20** in dammar and **18**/**22**, **20**/**23** in mastic with EI *m*/*z* 428, 472 and $NH_3$/CI *m*/*z* 446, 490 disappear after removal of the uppermost 15 μm in both cases. Since these particular compounds are only formed upon UV irradiation during accelerated aging [7], it is implied that the UV wavelengths of the incident light do not penetrate deeper than a 15 μm surface zone of the films. This observation was confirmed by MALDI-TOF-MS, which was performed by bringing ethanol wetted minute TLC plates coated with cellulose in contact with the surface of the laser processed films [25,42]. This finding is in agreement with the optical absorption lengths, $l_\alpha$, determined for the two aged TTP films and shows that both films completely absorb the ambient light with $\lambda < 350$ nm at depths shorter than 15 μm [15]. Moreover, the non-UV oxidized oleanane/ursane type compounds **25**–**28** in dammar and **25**, **26** in mastic (EI: *m*/*z* 234, 317, 414, 482; $NH_3$/CI:

**Table 3**
Data extracted from EI-DTMS total ion currents.

| Depth steps | Depth steps measured from surface (μm) | | Volatilization[a] (%) (normalized at scan no. of aged surface) | | % Pyrolysis yield[a] (%) (normalized at %area of aged surface) | |
|---|---|---|---|---|---|---|
| | Dammar | Mastic | Dammar | Mastic | Dammar | Mastic |
| Surface | 0 | 0 | 100 | 100 | 100 | 100 |
| 1 | 3.5 | 3 | 73 | 100 | 73 | 64 |
| 2 | 7 | 6 | 72 | 86 | 70 | 65 |
| 3 | 11.5 | 10 | 64 | 86 | 66 | 55 |
| 4 | 15 | 12 | 58 | 71 | 63 | 59 |
| 5 | 20 | 16 | 55 | 70 | 15 | 54 |
| 6 | 25 | 20 | 45 | 71 | 9 | 30 |
| 7 | – | 25 | – | 57 | – | 11 |
| Controls | 0 | 0 | 0 | 0 | 0 | 0 |

[a] The percentages derived by setting the scan no. of the volatilization peak apexes and the area integral of the pyrolysis peaks correspondingly for the aged samples as $X_{max}$ and the control samples as $X_{min}$ using the formula: $100\{(X - X_{min})/(X_{max} - X_{min})\}$, where $X$ was the respective value at each depth-step sample.

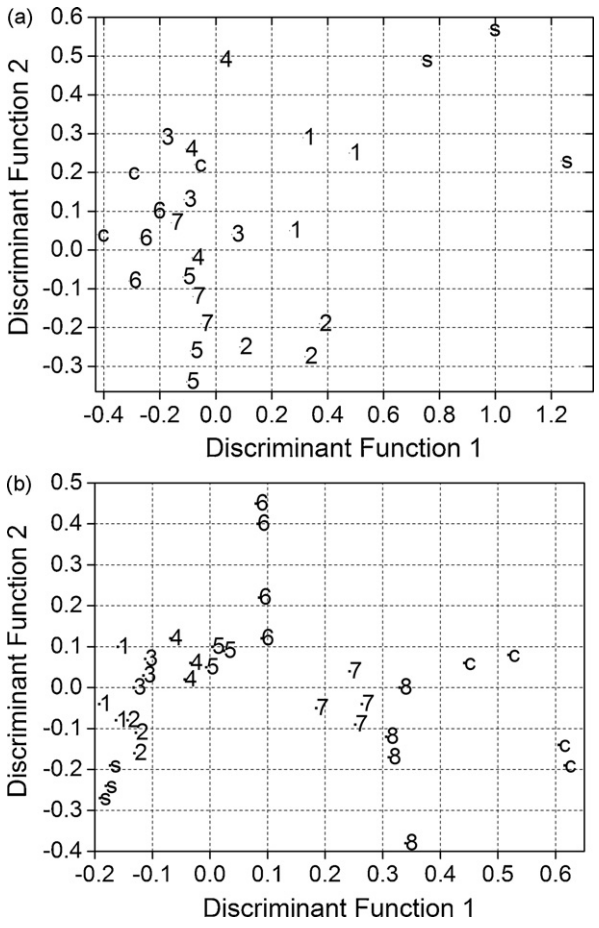


**Fig. 10.** MF-DA score maps of the DTMS across the dammar (a) and mastic (b) depth steps. The ascending numbers represent the compositions of the successive laser ablated depth steps. Data points number (s) correspond to the aged surfaces, while (c) to the controls. The consecutive shifts across the DF1 from the deteriorated surfaces towards the less deteriorated bulk are evident.

*m*/*z* 432, 458, 486) [2,4,31] also seem to reduce with depth in both cases.

The changes in molecular composition are also monitored by the gradual recovery of the abundances of the ion fragments corresponding to the unreacted dammarane (**3**–**7**) and oleanane/ursane type compounds (**1**, **2**, **8**–**12**) with depth. The compositional changes are less pronounced in the uppermost 15 μm, which absorb

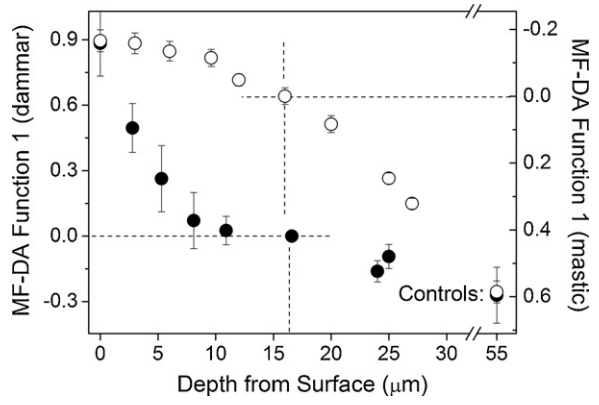


**Fig. 11.** MS projections of DF 1 as a function of depth in the 55-μm thick, aged dammar (●) and mastic (○) films. At approximately 15 μm the DTMS spectra corresponded to the DF1 origin in both cases, implying that this was the threshold between highly and less deteriorated material in both cases.

highly the UV wavelengths of the incident light. Strong molecular differences between surface and deeper parts of the films are observed beneath the highly deteriorated surface layers, especially in the case of dammar, where at depth of 20 μm the characteristic ion fragments of the unreacted compounds produce relative intensities comparable to those prior to aging (Fig. 6). At a 25 μm depth in the bulk of the aged mastic film the ion peak *m*/*z* 143, the ion fragment of the ocotillone molecules, i.e., **7**, decreases (Fig. 7), indicating that the dammarane type molecules and their oxidation products influence the composition of mastic less than that of dammar, as observed elsewhere [2,4,10]. In all, the molecular changes across the depth profiles of the aged films demonstrate that the composition is gradually shifting towards a less deteriorated state with increasing depth. At a depth of 20–25 μm the composition of the films resembles the composition prior to aging.

### *3.4. Multivariant factor discriminant analysis (MF-DA) of the DTMS data across the depth profiles of the aged dammar and mastic films*

Fig. 10 presents the plots of the MS data points as coordinates in the score map of the MF-DA analysis. The geometric distance between the MS data points along the discriminant functions (DF) 1 and 2 is an accepted measure of compositional differences [32,43]. The gradual shifts across DF1 correspond to the compositional gradient observed in the DTMS mass spectra. The data points from low to higher numbers correspond to the consecutive depth steps from the surface (s) towards the bulk, while the highest numbers represent the MS data of the control resins (c).

Fig. 11 shows the data points along DF1 plotted versus the depth profile of the two aged TTP films. Both cases reveal a remarkable compositional gradient. The results quantify the molecular modifications observed by DTMS. Although the gradients of the aged dammar and mastic films are not exactly the same, there is a very significant common characteristic. MF-DA analysis placed the origin of DF1 coordinate at approximately 15 μm below the deteriorated surfaces, indicating that this particular depth is threshold between highly and less deteriorated material. At this depth the pyrolysis peak of the DTMS-TIC curves is also reduced (Fig. 4) while there was also a noticeable change in the ablative photochemical interaction during the processing of the sampling steps by the KrF excimer laser [25]. This can be explained by the complete absorption of UV ambient light by the surface of the films as determined by UV/vis studies [15] and is in line with earlier indications, as described above [6,8,12,17]. The data points corresponding to the deepest depth steps (20–25 μm) plot near those of the control films. Given that the total film thicknesses were of the order of 55 μm, it is expected that at depths greater than 25 μm from surface the composition of the films would be similar to that prior to aging.

## 4. Conclusions

This paper is a direct-temperature mass spectrometric study across the depth profiles of accelerated aged dammar and mastic films that were uncovered by optimized KrF excimer laser ablation (248 nm, 25 ns). The results establish on the molecular level the generation of depth-dependent compositional gradients in triterpenoid resins as a result of aging. Electron ionization DTMS total ion currents show that the temperature required to volatilize the polar compounds is reduced as analysis is performed to the films with their upper layer of increasing thickness being removed. The integrated area of the pyrolysis peak is also reduced with depth, indicating a depth-dependent decrease of the amount of high-MW material generated upon aging. DTMS in both EI and $NH_3$/CI ionization modes determine that relative abundances of known marker ions of oxidized dammarane, oleanane and ursane type

triterpenoids are gradually decreasing as a function of depth. In contrast, marker ion of unreacted TTP compounds increase with depth. In addition, DTMS analysis determines that UV-induced oxygenated TTP compounds, such as oleanane/ursane type molecules with oxidized A-rings, are only present in the 15-μm uppermost surface layers. Multivariant factor discriminant analysis, that quantified the molecular gradients as detected by the EI-DTMS sum spectra, determines that the depth of 15 μm from surface is the threshold between highly and much less deteriorated material in the TTP films. Below these layers, only non-UV oxidation products, such as oleanane/ursane TTP molecules with side-chain oxidation at positions C-11 and C-28, are detected. At depths of the order of 25 μm into the bulk the composition of both TTP resin films is similar to that of the control samples.

## Acknowledgements

The MS work at the FOM Institute for Atomic and Molecular Physics (AMOLF) in Amsterdam was supported by the FOM Program 49 funded by FOM and NWO (The Hague, The Netherlands). The work is further supported by the E.U. Cluster of Large Scale Laser Installations (LIMANS) Plan DGXII (HCM) program ERBCHGECT920007 at the Ultraviolet Laser Facility at FORTH-IESL in Heraklion, Greece. The authors thank J. van der Horst for his technical assistance at FOM-Institute AMOLF, Professor Dr. C. Fotakis for providing access to the Ultraviolet Laser Facility at FORTH-IESL and Dr. P. Argitis for providing access to the Institute of Microelectronics (IMEL), NCSR 'Demokritos', Athens, Greece, where spin-coating was performed. Accelerated aging was performed at the Courtauld Institute of Art, London, UK.

## References

[1] J.S. Mills, R. White, The Organic Chemistry of Museum Objects, 2nd ed., Butterworth-Heinemann, Oxford, 1994.
[2] G.A. van der Doelen, K.J. van den Berg, J.J. Boon, Stud. Conserv. 43 (1998) 249.
[3] G.A. van der Doelen, K.J. van den Berg, J.J. Boon, N. Shibayama, E.R. de la Rie, W.J.L. Genuit, J. Chromatogr. A 809 (1998) 21.
[4] G.A. van der Doelen, Ph.D. Thesis, University of Amsterdam, The Netherlands, 1999.
[5] E.R. de la Rie, Ph.D. Thesis, University of Amsterdam, The Netherlands, 1988.
[6] J.J. Boon, G.A. van der Doelen, Advances in the current understanding of aged dammar and mastic triterpenoid varnishes on the molecular level, in: A. Harmssen (Ed.), Firnis: Material-Aesthetik-Geschichte, International Kolloquium, Braunschweig, 1998, Hertog-Anton-Ulrich-Museum, Braunschweig, 1999, p. 92.
[7] G.A. van der Doelen, K.J. van den Berg, J.J. Boon, in: J.-P. Mohen (Ed.), Art Chimie: La Couleur: Actes du Congres, CNRS Editions, Paris, 2000, p. 146.
[8] E.R. de la Rie, Stud. Conserv. 33 (1988) 53.
[9] S. Zumbühl, R. Knochenmuss, S. Wülfert, F. Dubois, M.J. Dale, R. Zenobi, Anal. Chem. 70 (1988) 707.
[10] D. Scalarone, J. van der Horst, J.J. Boon, O. Chiantore, J. Mass Spectrom. 38 (2003) 607.
[11] J. Koller, U. Baumer, D. Grosser, E. Schmid, in: J. Koller (Ed.), Baroque and Rococo Lascquers, Arbeitshefte des Bayerischen Landesamtes fuer Denkmalpflege, vol. 81, Karl M. Lipp Verlag, München, 1997, p. 347.
[12] P. Dietemann, Ph.D. Thesis, Swiss Federal Institute of Technology, Zurich, 2003.
[13] J.S. Mills, A.E.A. Werner, J. Chem. Soc. (1955) 3132.
[14] B.L. Poehland, B.K. Carte, T.A. Francis, L.J. Hyland, H.S. Allaudeen, N. Troupe, J. Nat. Prod. 50 (1987) 706.
[15] C. Theodorakopoulos, V. Zafiropulos, J.J. Boon, S.C. Boyatzis, Appl. Spectrosc. 61 (2007) 1045.
[16] V. Zafiropulos, A. Manousaki, A. Kaminari, S.C. Boyatzis, ROMOPTO: Sixth Conference on Optics, SPIE, vol. 4430, Washington, 2001, p. 181.
[17] C. Theodorakopoulos, V. Zafiropulos, J. Cult. Herit. 4 (2003) 216.
[18] G. Thomson, Application of Science in Examination of Works of Art, Museum of Fine Arts, Boston, 1965, p. 78.
[19] G. Thomson, Natl. Gallery Tech. Bull. 3 (1979) 25.
[20] G. Thomson, Natl. Gallery Tech. Bull. 2 (1978) 66.
[21] A.V. Cunliffe, A. Davis, Polym. Degrad. Stab. 4 (1982) 17.
[22] T. Fukushima, Durability Build. Mater 1 (1983) 327.
[23] G.E. Schoolenberg, P. Vink, Polymer 32 (1991) 432.
[24] R.L. Feller, in: D. Berland (Ed.), Accelerated Aging: Photochemical and Thermal Aspects, The Getty Conservation Institute, USA, 1994, 56, 135.
[25] C. Theodorakopoulos, Ph.D. Thesis, RCA, London UK, with IESL/FORTH, Greece, and FOM-Institute AMOLF, The Netherlands, 2005.
[26] C. Theodorakopoulos, V. Zafiropulos, C. Fotakis, J.J. Boon, J. van der Horst, K. Dickmann, D. Knapp, in: K. Dickmann, C. Fotakis, J.F. Asmus (Eds.), Springer Proceedings in Physics, Vol. 100, Springer-Verlag, Berlin, Heidelberg, 2005, p. 255.
[27] M. Castillejo, M. Martin, M. Oujja, D. Silva, R. Torres, A. Manousaki, V. Zafiropulos, O.F. van den Brink, R.M.A. Heeren, R. Teule, A. Silva, H. Gouveia, Anal. Chem. 74 (2002) 4662.
[28] V.P. Papageorgiou, M.N. Bakola-Christianopoulou, K.K. Apazidou, E.E. Psarros, J. Chromatogr. A 769 (1997) 263.
[29] V. Zafiropulos, in: B.S. Luk'yanchuk (Ed.), Applied Physics and Material Science: Laser Cleaning, World Scientific, Singapure, New Jersey, London, Hong Kong, 2002, p. 343.
[30] C. Fotakis, D. Anglos, V. Zafiropulos, S. Georgiou, V. Tornari, Lasers in the Preservation of Cultural Heritage Principles and Applications, Taylor & Francis, New York, London, 2006.
[31] G.A. van der Doelen, J.J. Boon, J. Photochem. Photobiol. A 134 (2000) 45.
[32] R. Hoogerbrugge, S.J. Willig, P.G. Kistemaker, Anal. Chem. 55 (1983) 1710.
[33] J.J. Boon, Int. J. Mass Spectrom. Ion Processes 118/119 (1992) 755.
[34] F.-J. Marner, A. Freyer, J. Lex, Phytochemistry 30 (1991) 3709.
[35] J.S. Mills, J. Chem. Soc. (1956) 2196.
[36] E. Seoane, J. Chem. Soc. (1956) 4158.
[37] B.G.K. van Aarssen, H.C. Cox, P. Hoogendoorn, J.W. de Leeuw, Geochim. Cosmochim. Acta 54 (1990) 3021.
[38] K.J. van den Berg, J. van der Horst, J.J. Boon, O.O. Sudmeijer, Tetrahedron Lett. 39 (1998) 2645.
[39] G. Scott, Atmospheric Oxidation and Antioxidants, Elsevier Science Publishers B.V., Amsterdam, 1993.
[40] R. Srinivasan, B. Braren, Chem. Rev. 89 (1989) 1303.
[41] R. Srinivasan, in: J.C. Miller (Ed.), Laser Ablation: Principles and Applications, Springer Series of Material Science, vol. 28, Springer, Berlin, Heidelberg, 1994, p. 107.
[42] D. Scalarone, M.C. Duursma, J.J. Boon, O. Chiantore, J. Mass Spectrom. 40 (2005) 1527.
[43] W. Windig, J. Haverkamp, P.G. Kistemaker, Anal. Chem. 55 (1983) 81.